Transition Met Chem
DOI 10.1007/s11243-015-9939-9

DNA interactions, antitumor activities and radical scavenging properties of oxovanadium complexes with pyrazino[2,3-*f*][1,10]phenanthroline ligands

Pengfei Zeng[1] · Limin He[2] · Zhenfeng Ye[1] · Ning Yang[3] · Yulan Song[3] · Jiazheng Lu[1]

Received: 5 February 2015 / Accepted: 7 April 2015

Abstract Two unsymmetrical oxovanadium complexes [VO(satsc)(dpq)] (**1**) (satsc = salicylaldehyde thiosemicarbazone, dpq = pyrazino[2,3-*f*][1,10]phenanthroline) and [VO(hntdtsc)(dpq)] (**2**) (hntdtsc = 2-hydroxy-1-naphthaldehyde thiosemicarbazone) have been synthesized and characterized. Both complexes show strong interactions with calf thymus DNA through an intercalative model and can efficiently cleave pBR322 DNA after irradiation with light. Both complexes also exhibit high cytotoxicities against SH-SY5Y, MCF-7 and SK-N-SH cell lines. Complex **2** was found to have higher antitumor potency, DNA-binding affinity and DNA-cleaving ability than complex **1**. The abilities of these complexes to scavenge hydroxy radicals were evaluated.

Introduction

A number of transition metal complexes have been shown to have the ability to bind and cleave DNA, especially those with polyaromatic ligands [1–4].Vanadium exhibits various biological and physiological effects in the human body [3, 5–7]. Therefore, vanadium complexes have been investigated as drugs and found to have antitumor, antimicrobial and insulin-enhancing properties [4–6]. Many vanadium complexes are able to suppress the growth and spread of existing tumors by inhibiting tumor cell proliferation, inducing apoptosis and limiting the invasion and metastatic potential of neoplastic cells [7, 8]. For this reason, the DNA-binding and antitumor activities of oxovanadium complexes with multifunctional bridging ligands have been investigated [9, 10]. Among these, Schiff base complexes have exhibited significant activities with respect to DNA binding and cleavage [9, 11–14]. Schiff base ligands play an important role in the DNA-binding characteristics of their associated complexes, because of their electronic effects [15, 16]. In particular, a rigid aromatic system in the Schiff base structure can give better interactions with DNA, which is an important consideration in the design of new effective DNA-binding complexes [17]. Previously, we have studied the interactions of Schiff base oxovanadium complexes with CT-DNA and also their cytotoxicities against myeloma cells (Ag8.653) and gliomas cells (U251) assessed by MTT assay. We found that Schiff base ligands with larger aromatic or electron-withdrawing groups generally have better DNA-binding and antitumor activities [17–19].

In continuation of our precious work, two new oxovanadium complexes [VO(satsc)(dpq)] (**1**) (satsc = salicylaldehyde thiosemicarbazone, dpq = Pyrazino[2,3-*f*][1,10]phenanthroline) and [VO(hntdtsc)(dpq)] (**2**) (hntdtsc = 2-rhydroxy-1-naphthaldehyde thiosemicarbazone) have been synthesized and characterized by spectroscopic and physicochemical methods. The interactions of these complexes with CT-DNA have been investigated. Their photocleavage reactions with pBR 322 supercoiled plasmid

✉ Limin He
he791225@163.com

✉ Jiazheng Lu
lujia6812@163.com

[1] School of Pharmacy, Guangdong Pharmaceutical University, Guangzhou 510006, People's Republic of China

[2] Department of Pharmaceutical Engineering, School of Pharmacy, Guangdong Pharmaceutical University, Guangzhou 510060, People's Republic of China

[3] Department of Clinical Pathology, First Affiliated Hospital, Guangdong Pharmaceutical University, Guangzhou 510060, People's Republic of China

Published online: 09 September 2015

DNA were also investigated, and the cytotoxicities toward human breast cancer line (MCF-7) and human neuroblastoma cells (SH-SY5Y and SK-N-SH) were investigated by MTT (3-(4,5-dimethyl-2-thiazolyl)-2,5-diphenyl-2-H-tetrazolium bromide) assay. In addition, their hydroxyl radical scavenging properties were investigated.

Experimental

Materials and methods

All reagents and solvents were of AR grade and purchased commercially. $VO(acac)_2$ (acac = acetylacetonate) and 1,10-phenanthroline were used as purchased (AR grade). CT-DNA and pBR322 supercoiled plasmid DNA were obtained from Sigma Company (Guangzhou, China). Human breast cancer line (MCF-7) and human D cells (SH-SY5Y and SK-N-SH) were purchased from the Cell Bank of Type Culture Collection of the Chinese Academy of Sciences (Shanghai, China). MTT was purchased from Sigma. Tris buffer A (Tris = tris(hydroxylmethyl)aminom ethane) containing 5 mM Tris–HCl and 50 mM NaCl (pH 7.2) was used for absorption titration, fluorescence emission and viscosity experiments. Tris buffer B containing 50 mM Tris–HCl and 18 mM NaCl (pH 7.2) was used for the gel electrophoresis experiments. Buffer C (1.5 mM $NaHPO_4$, 0.5 mM NaH_2PO_4 and 0.25 mM Na_2H_2 EDTA [*N*,*N*'-1,2-ethanediylbis[*N*-(carboxymethyl)]glycine) (pH 7.0)] was used for thermal denaturation studies. All of the above buffer solutions were prepared using double-distilled water. A solution of CT-DNA in buffer A gave a ratio of UV absorbance at 260 and 280 nm of 1.8–1.9:1, indicating that the DNA was sufficiently free of protein [20, 21]. The DNA concentration per nucleotide was determined by absorption spectroscopy using the molar absorption coefficient (6600 $M^{-1}cm^{-1}$) at 260 nm [20, 22]. DNA stock solutions were stored at 4 °C and employed after no more than 3 days. Compounds were dissolved in dimethyl sulfoxide (DMSO) and diluted with buffer solution to the required concentrations prior to use. Solutions of compounds were freshly prepared 2 h prior to biochemical evaluation.

Microanalyses (C, H and N) were obtained using a PerkinElmer 240Q elemental analyzer. Electrospray mass spectra (ES-MS) were recorded on a LCQ system (Finnigan MAT, USA) using methanol as mobile phase. ^{1}H NMR spectra were recorded on a Varian-500 spectrometer. All chemical shifts are given relative to tetramethylsilane (TMS). Infrared spectra were recorded on a Bomem FTIR model MB102 spectrometer using KBr pellets. UV–Vis spectra were recorded on a Shimadzu UV-3101 PC spectrophotometer at room temperature. Emission spectra were recorded on a PerkinElmer Lambda 55 spectra fluorophotometer. Cell assays were performed with a microplate reader (model 680, Bio-Rad, USA).

Synthesis of satsc

satsc was synthesized through a method similar to that described earlier. [17] A stirring solution of salicylaldehyde (1.2212 g, 10 mM) in 10 mL of absolute EtOH was added dropwise to a solution of thiosemicarbazide (0.9114, 10 mM) in absolute EtOH (15 mL). The mixture was continuously stirred at 80 °C for 3 h to give a white precipitate, which was used without further purification. Yield: 56 %. Anal. Calcd. For $C_8H_9N_3OS$: C, 49.2; H, 4.6; N, 21.5; S, 16.4 %; Found: C, 49.1; H, 4.7; N, 21.5; S, 16.4 %. ES-MS (CH_3OH, *m*/*z*): 196.0 (100 %) ($[M+1]^+$). IR (KBr) (ν_{max}/cm): 3444 (vs), 3321 (vs, $-NH_2$), 3175(vs, N–H), 3033 (m, C–H), 1617 (vs, C=N), 1537 (vs), 1491 (s), 1465 (s), 1237 (m, C–O), 1036 (m, C–N), 830 (s), 752 (s, C=S).^{1}H NMR (500 MHz, DMSO-d_6): 11.40 (s, 1H, NHCS), 9.89 (s, 1H, OH), 8.38 (s,1H, CH=N), 7.92 and 8.13 (2br s, 1H each NH_2), 7.92 (s, 1H, ArH),7.21(t, 1H, ArH, $J = 8.4$ Hz), 6.88 (d, 1H, ArH, $J = 7.8$ Hz), 6.81 (t, 1H, ArH, $J = 8.2$ Hz).

Synthesis of hntdtsc

This compound was prepared using a similar procedure to that described for satsc, using 2-hydroxy-1-naphthaldehyde (1.7218 g, 10 mmol) in place of salicylaldehyde to give a light yellow precipitate, which was used without further purification. Yield: 84 %. Anal. Calcd. For $C_{12}H_{11}N_3OS$: C, 58.8; H, 4.5; N, 17.1; S, 13.1 %; Found: C, 58.7; H, 4.6; N, 17.1; S, 13.0 %. ES-MS (CH3OH, *m*/*z*): 246.0 (100 %) ($[M+1]^+$). IR (KBr) (ν_{max}/cm^{-1}): 3450 (vs), 3253 (vs, $-NH_2$), 3167 (vs, N–H), 3053 (m, C–H), 1625 (s, C=N), 1593 (vs), 1572 (s), 1509 (vs), 1472 (s), 1452 (m), 1033 (m, C–N), 1240 (s, C–O), 821 (s), 753 (s, C=S). ^{1}H NMR (500 MHz, DMSO-d_6): 11.42 (s, 1H, NHCS), 10.51 (s, 1H, OH), 9.06 (s, 1H, CH=N), 7.85 and 8.25 (2br s, 1H, NH_2), 8.53 (d, 1H, ArH, $J = 8.7$ Hz), 7.89 (d, 1H, ArH, $J = 7.6$ Hz), 7.86 (d, 1H, ArH, $J = 8.2$ Hz), 7.57 (t, 1H, ArH, $J = 8.0$ Hz), 7.38 (t, 1H, ArH, $J = 7.6$ Hz), 7.21 (d, 1H, ArH, $J = 8.4$ Hz).

Synthesis of dpq

dpq was synthesized through a modification of a reported procedure [23]. To a solution of 1,10-phenanthroline-5,6-dione in water was added 1,2-ethanediamine, and the resulting suspension was refluxed for 12 h at 60 °C. The product was collected and washed with water (10 mL) and the minimum volume of diethyl ether. Yield: 68.7 %. Anal.

Calcd. For $C_{14}H_8N_4$: C, 70.4; H, 3.5; N, 24.1 %; Found: C, 70.4 H, 3.5; N, 24.1 %. ESI–MS (CH_3OH, *m/z*): 233.0($[M+1]^+$). IR (KBr) (ν_{max}/cm^{-1}):3000(m, =CH), 1581(m, C=N), 1571(m), 1519(m), 1467(s, C–H), 1390 (vs), 1078 (s), 804 (s), 740 (vs). ^1H NMR (500 MHz, DMSO-d_6): 9.46 (dd, 2H, $J = 10.25, 2.25$), 9.24 (dd, 2H, $J = 5.375, 2.25$), 9.19 (s, 2H), 7.96 (dd, 2H, $J = 10.25, 5.375$).

Synthesis of complex 1

A mixture of satsc (0.0975 g, 0.5 mmol) and dpq (0.116 g, 0.5 mmol) in absolute MeOH (15 mL) was refluxed under argon. After dissolution, a solution of $VO(acac)_2$ (0.1325 g, 0.5 mmol) in MeOH (10 mL) was added dropwise to the refluxing solution. A brown precipitate was formed after refluxing for another 4 h. The precipitate was collected by filtration, washed with absolute methanol and then dried in vacuo. Yield: 82.6 %. The crude product was purified by recrystallization such that the material was dissolved in hot MeOH and cooled to room temperature; whereupon the pure product precipitated out. Anal. Calcd. For $C_{22}H_{16}N_7O_2SV$: C, 53.6; H, 3.3; N, 19.9; O, 6.5; S, 6.5; V, 10.3 %; Found: C, 53.6 H, 3.3; N, 19.9; O, 6.5; S, 6.5; V, 10.4 %. ES-MS (CH_3OH, *m/z*): 493.05 (100 %) ($[M+1]^+$). IR (KBr) (ν_{max}/cm^{-1}): 3436 (s), 3290 (s, $-NH_2$), 3113 (m, C-H), 1601 (vs, C=N), 1540 (s), 1507 (s), 1469 (s), 1207 (m, C–O), 1151 (m, C–N), 940 (s, VO), 815 (m), 734 (m, C–S), 599 (m). ^1H NMR (500 MHz, DMSO-d6): 9.03 (s, 1H, CH=N), 7.82 (br, m, 3H), 7.53–7.35 (br m, 6H), 7.20 (2H, NH_2).

Synthesis of complex 2

Complex **2** was synthesized by a similar procedure as for the complex **1**, using hntdtsc (0.123 g, 0.5 mmol) in place of satsc. The precipitate was reddish brown. Yield: 81.2 %. The recrystallization procedure was same as for complex **1**. Anal. Calcd. For $C_{26}H_{18}N_7O_2SV$: C, 57.46; H, 3.34; N, 18.04; O, 5.89; S, 5.90; V, 9.37; Found: C, 57.48 H, 3.36; N, 18.07; O, 5.89; S, 5.88; V, 9.39 %. ES-MS (CH_3OH, *m/z*): 543.07 (100 %) ($[M+1]^+$). IR (KBr) (ν_{max}/cm^{-1}): 3332 (s, NH_2), 3193 (m), 2963 (m, C–H), 1614 (s, C=N), 1597 (s), 1537 (vs), 1499 (s), 1193 (m, C–O), 1085 (m, C–N), 956 (s, VO), 811 (s), 732 (m, C–S). ^1H NMR (500 MHz, DMSO-d6): 9.33 (s, 1H, CH=N), 7.87 (br, m, 3H), 7.57–7.34 (m, 6H), 7.20 (2H, NH_2).

DNA-binding studies

DNA-binding experiments were performed at room temperature. Absorption titrations of the complexes in buffer A were performed by using a fixed concentration of oxovanadium complex (20 μM) to which the DNA stock solution was added. The resulting mixtures were allowed to incubate for 5 min before the absorption spectra were recorded. In order to further elucidate the binding strength of the complexes, values of the intrinsic binding constant K_b with CT-DNA were obtained by monitoring the change in the absorbance of the ligand transfer band with increasing amounts of DNA. The data were then fitted to the following equation to obtain the value of K_b [17–20].

$$\frac{[DNA]}{\varepsilon_a - \varepsilon_f} = \frac{[DNA]}{\varepsilon_b - \varepsilon_f} + \frac{1}{K_b(\varepsilon_b - \varepsilon_f)}$$

where [DNA] is the concentration of DNA in the base pairs and ε_a, ε_f and ε_b refer to the corresponding apparent absorption coefficient A_{obsd}/[vanadium], the extinction coefficient for the free oxovanadium complex and the extinction coefficient for the oxovanadium complex in the fully bound form, respectively. Plots of $[DNA]/(\varepsilon_a - \varepsilon_f)$ versus [DNA] yielded values of K_b by the ratio of the slope to the intercept.

Viscosity and thermal denaturation experiments

The viscosity experiments were conducted using an Ubbelohde viscometer, immersed in a thermostatic water bath maintained at a constant temperature (28.0 ± 0.1) °C. A digital stopwatch was used for measurement of flow times, and each sample was measured five times to obtain the average flow time. Data are presented as $(\eta/\eta_0)^{1/3}$ versus binding ratio, where η is the viscosity of DNA in the presence of the complex, while η_0 is the viscosity of DNA alone [17, 25, 26].

DNA-melting experiments were done by monitoring the absorption intensity of CT-DNA (80 μM) at 260 nm at various temperatures, both in the absence and in the presence of the complexes (10 μM). Measurements were taken using a Shimadzu UV-3101 PC spectrophotometer attached to a Peltier temperature controller by increasing the temperature of the solution by 5 °C per min from 50 to 90 °C.

DNA photocleavage studies

The DNA cleavage activities of the complexes were assayed by agarose gel electrophoresis. Supercoiled plasmid pBR322 DNA (0.1 μg) was treated with the required complex in buffer B, and the solution was incubated at 37 °C. The samples were analyzed by electrophoresis for 1.5 h at 81 V on 0.8 % agarose gel in TBE (89 mM Tris–borate acid, 2 mM EDTA, pH 8.3). The gel was stained with 1 μg/mL ethidium bromide and photographed on an Alpha Innotech IS-5500 fluorescence chemiluminescence and visible imaging system. The efficiency of DNA cleavage was measured by determining the ability of the

complex to form open circular or nicked circular DNA from its supercoiled form [17, 20–24].

Cytotoxicity assays

The abilities of the complexes to interfere with the growth of SH-SY5Y, MCF-7 and SK-N-SH human cancer cell lines were determined by the 3-(4,5-dimethylthiazol-2-yl)-2,5 diphenyltetrazolium bromide (MTT) dye assay. Compounds were dissolved in 0.1 % DMSO and diluted with RPMI 1640 to the required concentrations prior to use [25–30]. A control well was prepared by the addition of culture medium (100 μL). Wells containing culture medium without cells were used as blanks. SH-SY5Y, MCF-7 and SK-N-SH cells with a density 2×10^4 cells per well were precultured into 96-well microtiter plates for 48 h at 37 °C in a 5 % CO_2 incubator. On completion of the incubation, stock MTT dye solution was added to each well. After 4-h incubation, a solution containing *N*,*N*-dimethylformamide (50 %) and sodium dodecyl sulfate (20 %) in water was added to solubilize the MTT formazan. The cell viability was determined by measuring the absorbance of each well at 490 nm using a Multiskan ASCENT microplate reader. IC_{50} values were determined by plotting the percentage viability versus concentration on a logarithmic graph and reading off the concentration at which 50 % of cells remained viable relative to the control [25, 29–32].

Radical scavenger measurements

Hydroxyl radicals were prepared in aqueous media using the Fenton system [33]. A solution of each complex was prepared with DMF (*N*,*N*-dimethylformamide). Each 4 mL aliquot of assay mixture contained the following reagents: the test compound (2.0–5.0 μM), safranin (28.5 μM), EDTA-Fe(II) (100 μM), H_2O_2 (44.0 μM) and phosphate buffer (67 mM, pH 7.4). The absorbance of the assay mixture was measured at 520 nm after incubation at 37 °C for 15 min in a water bath. All tests were run in triplicate and are expressed as the mean. The absorbance in the presence of the test complex A_i, the absorbance in the absence of the complex A_0 and the absorbance in the absence of the test complex and EDTA-Fe(II) A_C were measured. The scavenging ratio (%) was calculated using the following equation [34].

$$(A_i - A_0)/(Ac - A_0) \times 100\ \%$$

The data are expressed as the mean ± SD from these independent experiments. Statistical analysis was performed using SPSS 13.0 for Windows. Comparisons between the two groups were performed using an unpaired *t* test. Multiple comparisons between more than two groups were performed by one-way analysis of variance (ANOVA). Significance was accepted at a *P* value lower than 0.05.

Results and discussion

Synthesis and characterization

The free ligands satsc and hntdtsc were prepared by the reaction of thiosemicarbazide with 2-hydroxy-1-naphthaldehyde and salicylaldehyde, respectively. Complexes **1** and **2** were prepared by refluxing a mixture of the required ligand, $VO(acac)_2$ and dpq in absolute methanol, and then purified by recrystallization. The structures of the complexes were deduced by elemental analysis, ES-MS, UV–Vis, IR and ^1H NMR spectroscopy. The syntheses of the free ligands and their complexes are summarized in Scheme 1.

The IR spectra of the free Schiff bases were compared with the spectra of their oxovanadium complexes. The frequency of absorption of the azomethine (–CH=N) group was reduced by 16 and 11 cm^{-1} for complexes **1** and **2,** respectively. A signal for the V–S bond was observed for complexes **1** and **2** at 733 and 732 cm^{-1}, respectively, and V–O stretching for the complexes occurred at 940 and 956 cm^{-1}, respectively, as reported for other oxovanadium complexes. The ^1H NMR spectra of the free ligands were recorded in DMSO-d_6, and their tentative assignments are given in the experimental section. All the proton and carbon signals were observed in the expected regions.

The electronic spectra of the oxovanadium complexes and the free ligands are reported in the experimental section. The ESI–MS spectra of the free Schiff bases (satsc and hntdtsc) and dpq showed peaks at *m*/*z* 196 $[M+H]^+$, 216.0 $[M+H]^+$ and 233.0 $[M+H]^+$, respectively. The oxovanadium complexes ([VO(satsc)(dpq)] and [VO(hntdtsc)(dpq)]) gave peaks at *m*/*z* 493.0 $[M+H]^+$ and 543.0 $[M+H]^+$, respectively.

DNA-binding studies

Electronic absorption spectroscopy is one of the most common ways to investigate the interaction of complexes with DNA. The intercalation of complexes into the base pairs of DNA usually results in hypochromism and bathochromism (red shift) in the MCCT and ligand bonds, which is correlated with the stacking interaction between the planar aromatic chromophore of the complexes and the base pairs of DNA. The extent of the hypochromism is commonly consistent with the strength of the intercalative binding [17–20]. Figure 1 shows the absorption spectra of complexes **1** and **2** in the presence of increasing concentrations of DNA. Thus, upon increasing the CT-DNA

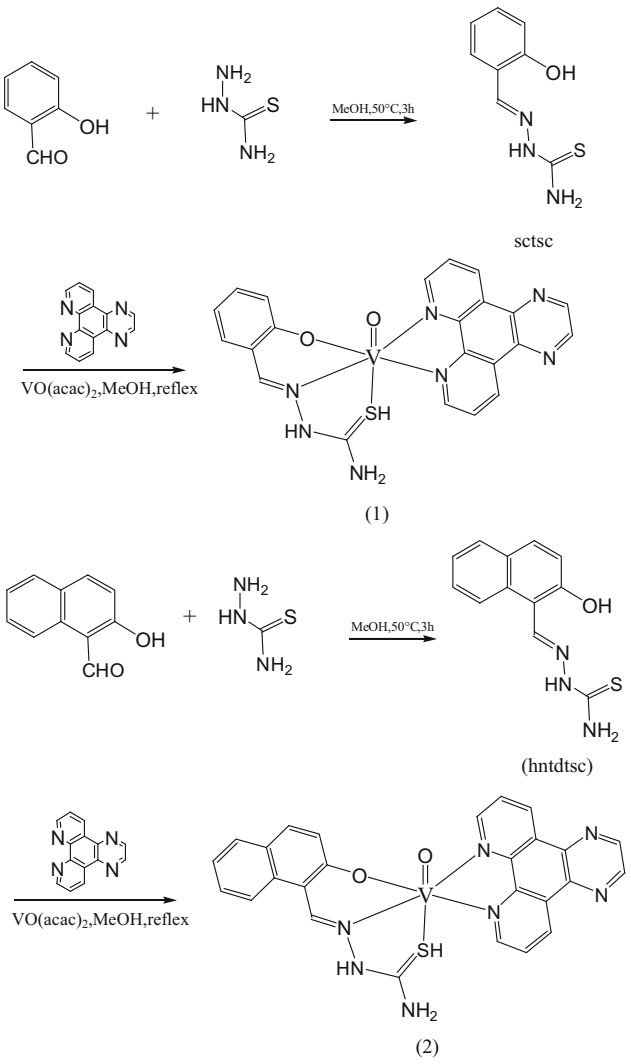

Scheme 1 Synthesis of ligands and complexes

concentration, the absorption band of complex **1** at 275 nm exhibited hypochromism of 15.9 % and bathochromism of about 3 nm. Complex **2** also exhibited hypochromism of 19.2 % at 263 nm and bathochromism of about 5 nm. These observations suggest that both oxovanadium complexes interact with DNA, most likely through a stacking mode between the aromatic chromophore and the base pairs of DNA.

The intrinsic binding constants K_b were calculated by monitoring the changes in absorbance of the ligand transfer bands with increasing amounts of CT-DNA. The values of K_b obtained for complexes **1** and **2** were 9.87×10^3 and 11.0×10^4 M^{-1}, respectively. The differences in their binding strengths may be due to the presence of an extra aromatic moiety in hntdtsc, resulting in larger binding affinities of the corresponding complexes compared to those of satsc.

The interaction of the complexes with CT-DNA was also studied using fluorescence emission titration experiments in Tris buffer A at room temperature. The emission spectra of the complexes in the absence and presence of CT-DNA are shown in Fig. 2. The maximum emission intensities were observed at 704 and 705 nm for complexes **1** and **2**, respectively. With increasing concentrations of CT-DNA, the emission intensities of complexes **1** and **2** increase by factors of about 1.36 and 1.24, respectively. The emission intensities of complexes **1** and **2** grow to about 13.3 and 12.2 % larger than those in the absence of DNA. The results indicate that both complexes can intercalate into the base pairs of the DNA and so be protected from the surrounding water molecules, thus lengthening their luminescence lifetimes. Our experiments also showed that there is a competition between ethidium bromide and the complexes for DNA binding.

Next, the interactions between the complexes and DNA were investigated by viscosity measurements. A classical intercalative mode is expected to cause a significant increase in the viscosity of the DNA solution due to an increase in the separation of base pairs at the intercalation sites and hence an increase in the overall DNA length. In contrast, a partial, non-classical intercalation of the ligand could bend (or kink) the DNA helix and reduce its effective length and, concomitantly, its viscosity [26].

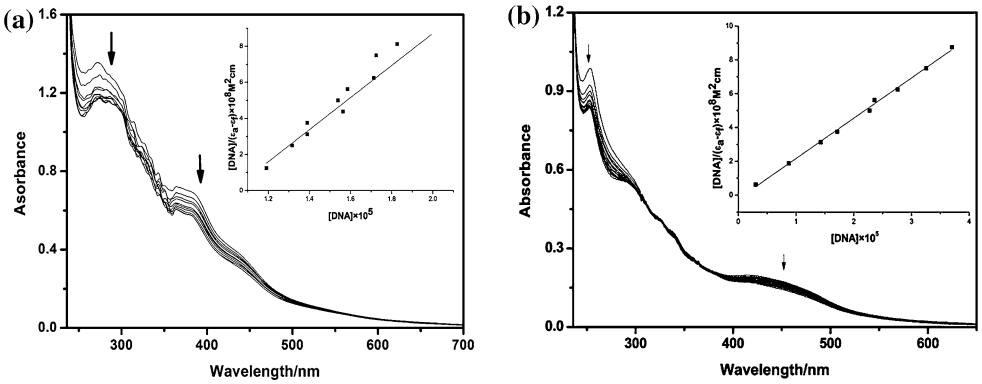

Fig. 1 Absorption spectra of the complexes **1**(**a**) and **2**(**b**) in Tris–HCl buffer I upon increasing amounts of CT-DNA. [V] = 20 μM, [DNA] = (0–100) μM. *Arrow* shows the decrease upon increasing CT-DNA concentrations. *Inset* plots of $[DNA]/(\varepsilon_a - \varepsilon_f)$ versus [DNA] for the titration of [V] with CT-DNA

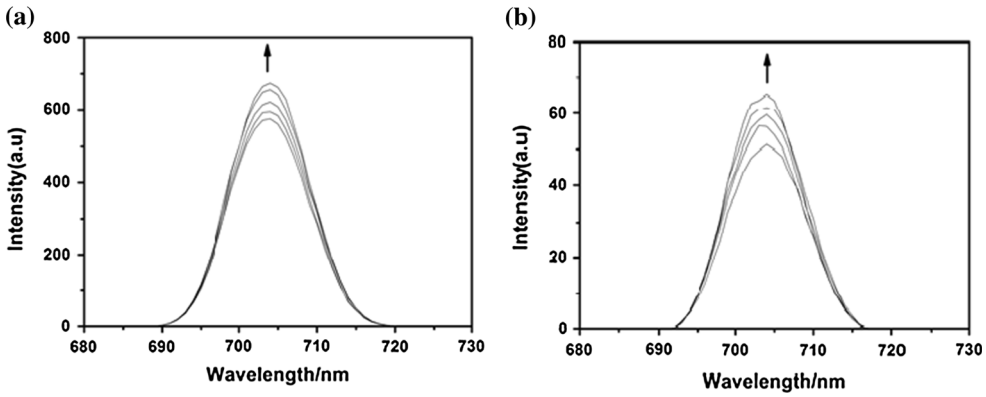

Fig. 2 Emission spectra of complexes **1**(**a**) and **2**(**b**) in Tris–HCl buffer 1 in the absence and presence of CT-DNA. [V] = 20 μM. *Arrows* shows increasing intensity upon increasing DNA concentration

The effects of addition of EB and complexes **1** and **2** on the CT-DNA viscosity are shown in Fig. 3. Upon increasing the amounts of complexes **1** and **2**, the relative viscosity of DNA increases steadily. EB, as a typical intercalator, also increases the relative DNA viscosity [24, 25, 27]. These results are in agreement with the above UV spectroscopic data and provide strong evidence for the interaction of complexes **1** and **2** with DNA by intercalative binding. The electronic effect of phenanthroline appears to be an important factor in determining the intrinsic binding constant K_b.

Thermal denaturation experiments have been carried out in order to explore the binding of the complexes with CT-DNA. As Fig. 4 shows, a small positive shift of DNA-melting temperature (ΔT_m) is observed on addition of the complexes to CT-DNA. In contrast to the above results, the low ΔT_m values for **1** and **2** suggest primarily groove binding of the complexes to CT-DNA stabilizing the DNA double-helix structure, in preference to an intercalative mode of binding to DNA that normally gives a large positive ΔT_m value [17–20, 24].

DNA cleavage experiments

The cleavage reactions of the complexes with plasmid DNA were monitored by agarose gel electrophoresis. Both complexes showed considerable DNA cleavage ability at low concentrations (15 μM) in the presence of H_2O_2. When circular plasmid DNA is subject to electrophoresis, relatively fast migration will be observed for the intact supercoiled form (form I). If scission occurs on one strand (nicking), the supercoil form will relax to generate a slower-moving open circular form (form II). If both strands are cleaved, a linear form (form III) that migrates between forms I and II will be generated [26, 27].

Figure 5 shows the cleavage of plasmid pBR332 DNA after incubation with complexes **1** and **2** at 37 °C for 1 h in the dark. There was no cleavage of pBR 322 DNA for H_2O_2 alone under the same conditions, as shown in lane 2. In the presence of complexes **1** and **2** with 30 mM L^{-1} H_2O_2 (lanes 3–5 and 8–10, respectively) or 30 mM H_2O_2 and 0.02 M L-histidine as a singlet oxygen quencher (lanes 6 and 11), plasmid DNA was nicked as is evident from the

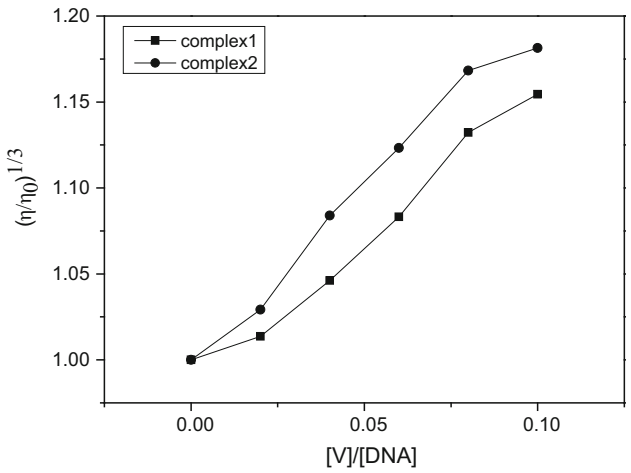

Fig. 3 Effects of increasing the amounts of complexes **1** and **2** on the relative viscosity of CT-DNA at 28 (±0.1) °C. [DNA] = 0.40 Mm

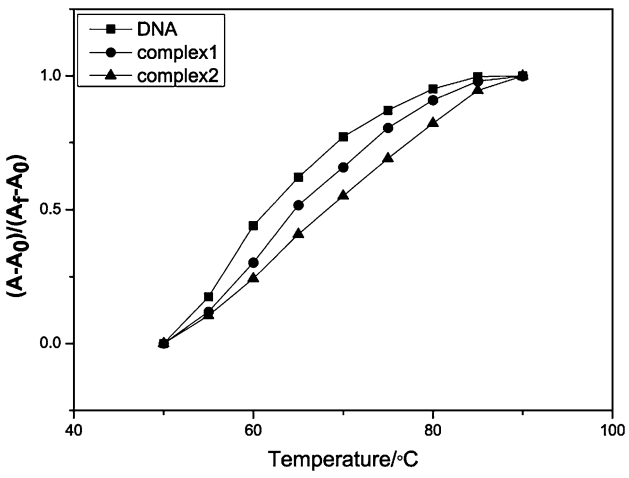

Fig. 4 Thermal denaturation of CT-DNA in the absence (*filled square*) and presence of complexes **1** (*filled circle*) and **2** (*filled triangle*). [V] = 20 μM, [DNA] = 80 μM

formation of form II, while L-histidine slightly inhibits the cleavage of DNA. Conversely, in the presence of the hydroxyl radical scavenger DMSO (lanes 7, 12), complete inhibition of DNA cleavage occurred, which suggests that ·OH radical is likely to be the reactive species for cleavage. This can be explained by the generation of ·OH radicals obtained from the oxidation of VO^{2+} in the presence of H_2O_2 through the following reaction:

$$VO^{2+} + H_2O_2 \rightarrow VO^{+} + \cdot OH + H^{+}$$

According to previous reports, the process of DNA cleavage may be closely related to oxidation of vanadyl ions in the presence of H_2O_2.

Cytotoxicity assays in vitro

The antitumor activities of the two complexes and the corresponding free ligands against SH-SY5Y, MCF-7 and SK-N-SH cell lines were evaluated by MTT assay [28–30]. The IC_{50} values of the free ligands and their complexes against these tumor cells after continuous exposure for 48 h are shown in Table 1.

As shown in Table 1, the complexes exhibit broad inhibition of all three human cancer cell lines with IC_{50} values ranging from 3.48 to 26.34 μM. The SK-N-SH cells proved to be the most sensitive to treatment with these complexes. Micrographs of the SH-SY5Y cell lines after treatment for 48 h in the absence (I) and presence of complexes **1** (II) and **2** (III) are shown in Fig. 6.

In Table 1 and Fig. 6, it can be seen that the complexes and free ligands all showed cytotoxicity against the three tumor cell lines [30–32]. The two oxovanadium complexes were more cytotoxic than the free ligands. Complex **2** shows the most potent inhibitory effect against these cell lines. This is consistent with its binding abilities with CT-DNA, indicating that the antitumor abilities of the oxovanadium complexes may be related to their interactions with DNA. These results are in line with our previous studies [17–20, 25]. However, the detailed mechanism of the antiproliferative effect of these complexes on cancer cells will require further study.

Table 1 The IC_{50} values for complexes and ligands against SH-SY5Y, SK-N-SH and MCF-7 cell lines

Compounds	IC_{50}* (μM)		
	SH-SY5Y	MCF-7	SK-N-SH
Cisplatin	7.72 ± 0.24	13.36 ± 1.25	2.95 ± 0.14
dpq	14.04 ± 0.65	29.34 ± 4.23	8.67 ± 0.63
hntdtsc	23.79 ± 2.15	>100	4.67 ± 0.63
satsc	49.53 ± 4.21	>100	33.98 ± 1.23
$VO(acac)_2$	43.61 ± 1.54	>100	20.78 ± 1.54
VO(satsc)(dpq)	10.64 ± 0.21	26.34 ± 0.39	5.551 ± 0.025
VO(hntdtsc)(dpq)	8.30 ± 0.09	23.46 ± 1.27	3.48 ± 0.017

* Cells were treated with various concentrations of tested compounds for 48 h. Cell viability was determined by MTT, and IC_{50} values were calculated as described in "Materials and methods". Each value represents the mean SD of three independent experiments

Hydroxyl radical scavenging experiments

As one of the most important reactive oxygen species (ROS), hydroxyl radical can cause cell membrane disintegration, membrane protein damage and DNA mutations. The scavenging effect on hydroxy radical of complexes **1** and **2** was observed [33, 34]. Since complexes **1** and **2** showed good ability to cleave DNA, it was considered necessary to investigate their scavenging effects on the hydroxy radical. Rutin, which is known to be an effective antioxidant agent [35], was used as a positive control. As shown in Fig. 7, the scavenging effect of complexes **1** and **2** was concentration dependent. However, the scavenging ratio decreased when the concentration reached 4.0 μM. This may be attributed by the generation of ·OH radicals obtained from the oxidation of VO^{2+} in the presence of H_2O_2 through the following reaction [18, 25–28]:

$$VO^{2+} + H_2O_2 \rightarrow VO^{+} + \cdot OH + H^{+}$$

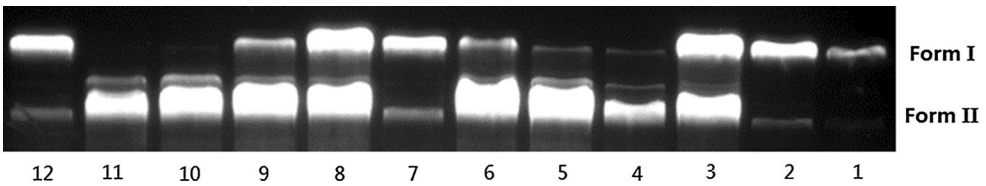

Fig. 5 Cleavage of pBR322 DNA by oxovanadium complexes **1** and **3** (15–60 μM) in the absence and presence of H_2O_2 (30 mM) in buffer B (pH 7.2). *Lane 1* DNA control; *lane 2* DNA + H_2O_2; *lane 3* DNA + 1(15 μM) +H_2O_2; *lane 4* DNA + 1(30 μM) + H_2O_2; *lane 5* DNA + 1(60 μM) + H_2O_2; *lane 6* DNA + 1(30 μM) + H_2O_2 + L-histidine (0.02 M); *lane 7* DNA + 1(30 μM) + H_2O_2 + DMSO (2μL); *lane 8* DNA + 3(15 μM) + H_2O_2; *lane 9* DNA + 3(30 μM) + H_2O_2; *lane 10* DNA + 3(60 μM) + H_2O_2; *lane 11* DNA + 3(30 μM) + H_2O_2 + L-histidine (0.02 M); *lane 12* DNA + 3(30 μM) + H_2O_2 + DMSO (2μL)

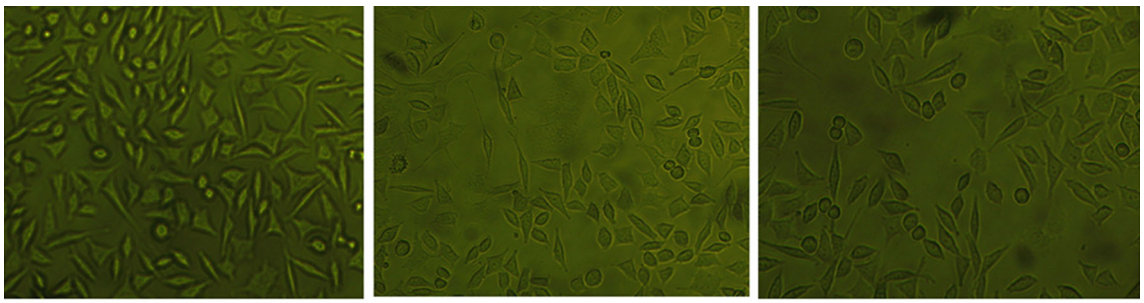

Fig. 6 Micrograph of the SH-SY5Y cell line after treated for 48 h in the absence (**I**) (control) and presence of same concentration (200 μM) of complexes **1** (**II**) and **2** (**III**), respectively

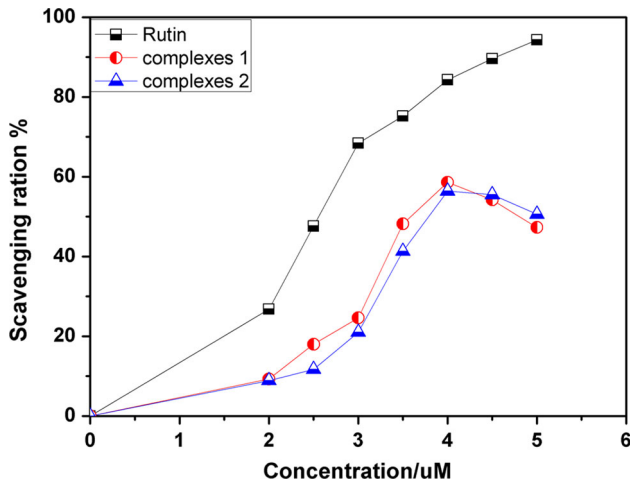

Fig. 7 Scavenging effect of the complexes on hydroxyl radicals

This phenomenon suggests that the oxovanadium complexes can scavenge hydroxy radicals and they can also be generated in the presence of H_2O_2. The detailed mechanism of this process requires further study.

Conclusion

Two oxovanadium complexes have been synthesized and characterized. Both complexes bind to CT-DNA by intercalation modes and show efficient oxidative cleavage of pBR 322 in the presence of H_2O_2. The complexes are toxic against human cancer cells (SH-SY5Y, MCF-7 and SK-N-SH) and also scavenge hydroxy radicals. These results may be of use in the further development of oxovanadium(IV) complexes as potential anticancer drugs.

Acknowledgments We gratefully acknowledge financial support for this work by the Science and technology Research Project of Guangdong Province (No. 2012B031800431), P. R. China, and Cultivation of Natural Science Joint Fund of the First Affiliated Hospital and the Scientific and Technical Department of Guangdong Pharmaceutical University (No. 2014-36).

Conflict of interest The authors have declared that there is no conflict of interest.

References

1. Liang JW, Wang Y, Du KJ, Li GY, Guan RL, Ji LN, Chao H (2014) J Inorg Biochem 141:17–27
2. Sreekanth B, Krishnamurthy G, Bhojyanaik HS, Gopinath SM, Vishnuvardhan TK, Shareef MI (2013) Int J Pharm Bio Sci 4:257–265
3. Naso LG, Lezama L, Rojo T, Etcheverry SB, Valcarcel M, Roura M, Salado C, Ferrer EG, Williams PAM (2013) Chem Biol Interact 206:289–301
4. Du SZ, Feng J, Lu XM, Wang G (2013) Dalton T 42:9699–9705
5. He GX, Xue LW, Zhao GQ (2013) Russ J Coord Chem 39:710–715
6. Sanna D, Micera G, Garribba E (2013) Inorg Chem 52:11975–11985
7. Benitez J, Becco L, Correia I, Leal SM, Guiset H, Pessoa JC, Lorenzo J, Tanco S, Escobar P, Moreno V, Garat B, Gambino D (2011) J Inorg Biochem 105:303–312
8. Maia PIS, Pavan FR, Leite CQF, Lemos SS, Gerimario F, Batista AA, Nascimento OR, Ellena J, Castellano EE, Niquet ED, Victor M (2009) Polyhedron 28:398–406
9. Liao XW, Pan WJ, He RW, Guo HW, Ying P, Lu JZ (2014) Chem Biol Drug Des 83:367–378
10. Banik B, Somyajit K, Nagaraju G, Chakravarty AR (2014) Dalton T 43:13358–13369
11. Selvamurugan S, Viswanathamurthi P, Endo A, Hashimoto T, Natarajan K (2013) J Coord Chem 66:4052–4066
12. Baluja S, Chanda S (2012) J Chem Biol Phys Sci 2:1176–1183
13. Garg G, Acharya A, Patel K (2013) Int J Biome Res 4:137–144
14. Kuz'min VE, Artemenko AG, Lozytska RN, Fedtchouk AS, Lozitsky VP, Muratov EN, Mescheriakov AK (2005) SAR QSAR Environ Res 16:219–230
15. Uno T, Hamasaki K, Tanigawa M, Shimabayashi S (1997) Inorg Chem 36:1676–1683
16. Pavan FR, Maia PIS, Leite SRA, Deflon VM, Batista AA, Sato DN, Franzblau SG, Leite CQF (2010) Eur J Med Chem 45:1898–1905
17. Lu JZ, Guo HW, Zeng XD, Zhang YL, Zhao P, Jiang J, Zang LQ (2012) J Inorg Biochem 112:39–48

18. Guo HW, Lu JZ, Ruan ZG, Zhang YL, Liu YJ, Zang LQ, Jiang J, Huang JW (2012) J Coord Chem 65:191–204
19. Lu JZ, Guo JW, Sang W, Guo HW (2013) Transit Metal Chem 38:481–488
20. Lu JZ, Du YF, Guo HW, Jiang J, Zeng XD, Zang LQ (2011) J Coord Chem 64:1229–1239
21. Kurita N, Kobayashi K (2000) Comput Chem 24:351–357
22. Rybkin VV, Tverdova NV, Girichev GV, Shlykov SA, Kuzmina NP, Zaitseva IG (2011) J Mol Struct 1006:173–179
23. Molphy Z, Prisecaru A, Slator C, Barron N, McCann M, Colleran J, Chandra D, Gathergood N, Kellett A (2014) Inorg Chem 53:5392–5404
24. Sasmal PK, Saha S, Majumdar R, Dighe RR, Chakravarty AR (2010) Inorg Chem 49:849–859
25. Liao XW, Pan WJ, He RW, Guo HW, Ying P, Lu JZ (2014) Chem Biol Drug Des 83:367–378
26. Wang JL, Zhao YQ, Yang BS (2014) Inorg Chim Acta 409:484–496
27. McCrate A, Carlone M, Nielsen M, Swavey S (2010) Inorg Chem Commun 13:537–539
28. Telpoukhovskaia MA, Cristina RR, Cawthray JF, Scott LE, Chris O (2014) Metallomics 6:249–262
29. Sgarbossa S, Diana E, Marabello D, Deagostino A, Cadamuro S, Barge A, Laurenti E, Gallicchio M, Boscaro V, Ghibaudi E (2013) J Inorg Biochem 128:26–37
30. Éva AE, Gabriella M, Bognár NVN, Tamás J, Tamás K, Dinorah G (2014) Polyhedron 67:242–252
31. Sinha A, Banerjee K, Banerjee A, Das S, Soumitra KC (2014) J Organomet Chem 772–773:34–41
32. León IE, Butenko N, DiVirgilio AL, Muglia CI, Baran EJ, Cavaco I, Etcheverry SB (2014) J Inorg Biochem 134:106–117
33. Li TR, Yang ZY, Wang BD, Qin DD (2008) Eur J Med Chem 43:1688–1695
34. Liao XW, Lu JZ, Ying P, Zhao P, Bai YL, Li WJ, Liu MP (2013) J Biol Inorg Chem 18:975–984
35. Pandurangan A, Ganapasam S (2008) Biomed Pharmacother 62(9):590–597